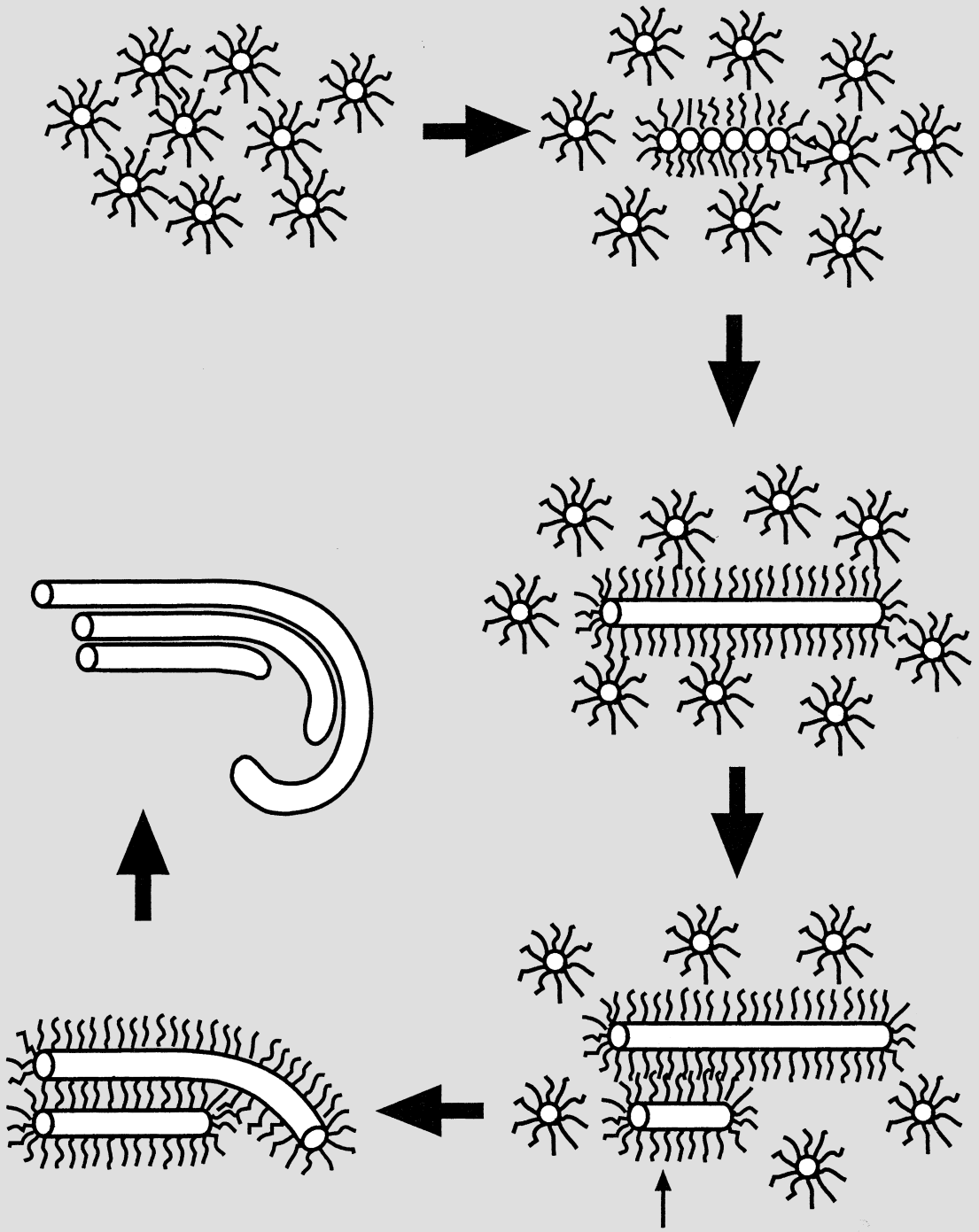

Synthesis of barium sulfate from surfactant – inorganic nanoparticles

The Chemistry of Form

Stephen Mann*

The emergence of complex form in living and nonliving systems remains a deep question for scientists attempting to understand the origins and development of shape and structure. In recent years, biologists and physicists have made significant advances in explaining fundamental problems in fields such as morphogenesis and pattern formation. Chemists, on the other hand, are only just beginning to contemplate the possibility of preparing manmade materials with lifelike form. This review traces a route to the direct synthesis of inorganic structures with biomimetic form, beginning from an understanding of crystal morphology and biomineralization. The equilibrium form of crystals can be modified by surface-active additives but only within limits dictated by the symmetry of the unit cell. In contrast, biological minerals, such as shells, bones, and teeth, are distinguished by a complexity of form that bears little resemblance to the underlying order of their inorganic crystals. By understanding the constructional processes that give rise to the inorganic structures of life it should be possible to develop a chemistry of form in the laboratory. For example, complex small-scale inorganic architectures are produced at room temperature by undertaking precipitation reactions in self-assembled organic media, such as surfactant micelles, block copolymer aggregates and microemulsion droplets. Unusual inorganic forms emerge when these reaction fields are subjected to instability thresholds and synthesis and self-assembly can be coupled to produce materials with higher-order organization. Like their biological counterparts, these hard inorganic structures represent new forms of organized matter which originate from soft chemistry.

Keywords: biomimetics · biomineralization · crystal growth · inorganic materials · morphology

1. Introduction

The notion of *form* has intrigued and inspired artists and philosophers since antiquity. In sculpture and architecture, form is more than spatial structure. It embodies aesthetics and metaphysical ideas such as the classical proportions of Greek and Roman architecture, humanism in Renaissance sculpture, and fluidity of shape in modern art. In sculpture, form emerges from the formless by the exclusion of matter—the carving of stone and wood, for example. Through this process, sculptors seek to release latent qualities of the material; a craft not dissimilar from that of the modern-day scientist who carves out nanofabricated patterns in the featureless terrain of a silicon wafer. Architecture in contrast is a bottom-up approach, in which building blocks are integrated into a spatial structure that has functional, aesthetic, and societal value. What sculpture is to physics, architecture is to chemistry.

[*] Prof. S. Mann
School of Chemistry
University of Bristol
Bristol BS8 1TS (UK)
Fax: (+44) 117-929-0509
E-mail: s.mann@bris.ac.uk

Nature, however, is indifferent to aesthetics, and survival of the genes through functional adaptation becomes an overriding principle in the appearance of biological form. What is so striking about the natural world is the remarkable level of morphological diversity and complexity, the seemingly endless variation of form in association with common functions. Trying to make sense of this is no easy task even though it is a central objective of palaeontology, and evolutionary and developmental biology. Prior to Darwin, natural form was studied with a metaphysical vigor to match the pursuit of sculpture and architecture. For example, German Naturphilosopie, as espoused by Ernst Haeckel (1834–1919), promulgated the coexistence of matter and spirit, and nowhere was this more exemplified than in the tiny ornate shells of single-celled organisms such as diatoms, coccoliths, and radiolarians (Figure 1).[1] This was contested by D'Arcy Thompson, whose book *On Growth and Form*[2] provided a compelling argument that natural form was simply the result of known physical and engineering principles applied to biological growth and development. In this paradigm, the inevitability of physical principles, such as space-filling and surface tension, could account for the general appearance of biological form, and geometric and topological perturbations to this blueprint paved the way to diversity. This view was also an affront to the

  1433-7851/00/3919-3393 $ 17.50+.50/0

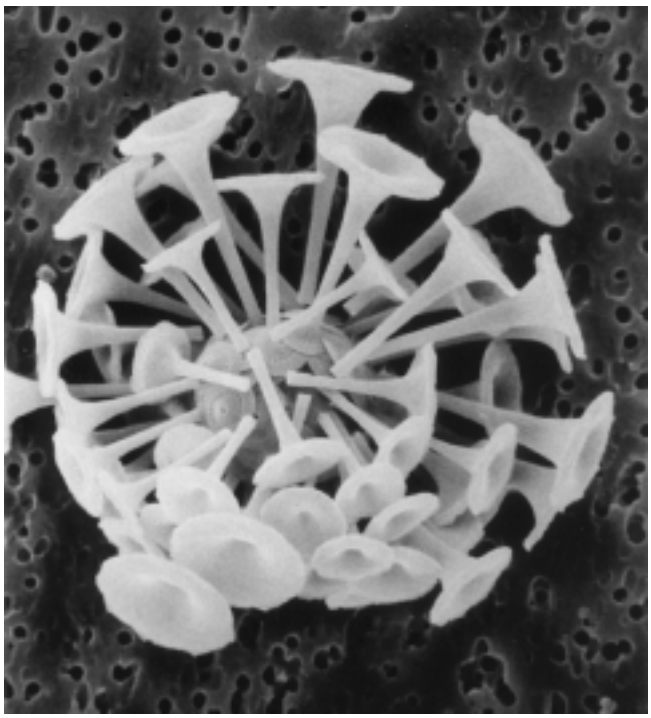

Figure 1. Natural form as expressed in the calcium carbonate exoskeleton of a marine coccolith (algae; diameter ca. 13 μm). (Photography courtesy of J. M. Young, Natural History Museum, London).

Darwinian theory of adaptation and natural selection, and although influential fell out of fashion as the culture of molecular biology developed in the late twentieth century.

The contention that biology is really just complicated physics is being currently reasserted as mathematical descriptions of self-organization become increasingly accessible. A wide range of natural patterns and forms—zebra stripes, butterfly wings, the structures of trees and lungs—can now be simulated and described by models based on fractal geometry and Turing waves.[3] What emerges is a view of form as a spatio-temporal process written in genetic code and subjected in part to the push-and-shove of physical contingency. The interplay and correlation of these factors produce a large gallery of potential forms that together describe the phylogenetic landscape of organisms.

The integration of mathematical (physical) and genetic (Darwinian) descriptions of natural form ultimately rests on an understanding of the mechanisms that transform the information coded in DNA into the expression of shape and pattern in time and space. The missing ingredient in this description is chemistry! For example, our knowledge of morphogenesis has increased rapidly in recent years because the activators and inhibitors have been identified at the molecular level and the processes that account for their secretion and spatial differentiation elucidated. Indeed, it is the patterning of chemical reactivity in localized space that appears to be central to the development of form.

If natural form is an emergent property of molecular processes then it should be possible for chemists to develop synthetic strategies that loosely mimic these processes. This review attempts to identify some ground rules for such an endeavor. We begin with the problem of form as described by structure, and then develop the notion of the equilibrium form of crystals and how geometric shapes are modified in the presence of surface-active molecules. Because the structural basis for crystal morphology contrasts markedly with the nonregularity but recognizable natural form of biominerals, the general principles of shape control in biomineralization are outlined. This leads to the question: how can an understanding of pattern formation in biomineral morphogenesis be integrated within a synthetic approach to inorganic materials with complex form? In response to this challenge, and as a starting point for future development, a conceptual framework for morphosynthesis is developed by using examples from recent investigations into the synthesis of inorganic materials in self-assembled reaction media.

2. Form as Description in Structure

Chemists on the whole focus on internal periodic order, and thus tend to neglect the richness and importance of external morphological form, even though soft matter and the natural world are replete in complex systems exhibiting aperiodicity,

Stephen Mann, born in 1955, is Professor in the School of Chemistry and Director of the Centre for Organized Matter Chemistry at the University of Bristol. He received his BSc. degree in chemistry from the University of Manchester Institute of Science and Technology (UMIST) in 1976, and was awarded a D.Phil. in 1982 from the University of Oxford for his work on biomineralization and bioinorganic materials chemistry. In 1981, he was elected to a Junior Research Fellowship at Keble College, Oxford, and took up a lectureship at the University of Bath in 1984 where he was promoted to reader in 1988, and appointed to a full professorship in 1990. His current research is concerned with biomimetic synthesis, as well as the characterization and emergence of complex forms of organized matter across extended length scales. He has obtained awards from the Royal Society of Chemistry (Corday-Morgan Medal in 1993, and RSC Interdisciplinary Award in 1999), is a recipient of the Max-Planck Research Prize for International Cooperation, awarded in 1998, and currently on the editorial and advisory board of numerous journals including Advanced Materials, Angewandte Chemie, *and* Chemistry of Materials. *He was admitted as a Fellow of the Royal Society of Chemistry in 1996.*

curvature, and hierarchy. However, there is a sense of wonder to be found in structural chemistry with its crystallographic databanks teeming with exquisite molecular contortions. But the nature of crystallinity forces us to reduce the breadth of form to a special subset concerned solely with the periodicity of unit cells. And in so doing, synthetic chemistry has effectively become trapped within the symmetry limitations of 230 space groups. The recent discovery of quasi-crystals with nonequivalent units represents a first step away from orthodox crystallography.[4] Ultimately this leads to a generalized study of order in soft matter[5]—vesicles, micelles, lipid tubules etc.—and an attempt to systematically describe the complexity of natural forms, such as trees, termite nests, human anatomy, etc, expressed in aperiodic hierarchical systems. Of course, it is not surprising that chemists remain enchanted with periodic order since it is so readily and elegantly elucidated by X-ray diffraction methods. And many structural challenges remain unresolved. For example, even simple crystal structures, such as calcium carbonate, have several polymorphic forms that are not readily predicted by ab initio methods. Indeed, it is debatable whether thermodynamics is the appropriate tool to extend the range of structure description, as local energy minima, activation energies, and reaction landscapes are likely to be responsible for the selection between polymorphs, particularly where differences in global energies at equilibrium are marginal. For instance, the vast number of zeolite structures of comparable free energies of formation can be attributed to kinetic selectivity induced by template-directed mechanisms during crystallization.[6]

The situation becomes even more complicated with the structural description of natural forms. Although these structures clearly retain a recognizable and reproducible pattern of order at the level of visual perception, they do not fit the crystallographers' *Weltanschauung* for several reasons. First, they are ordered but nonperiodic. Second, curvature is an integral aspect of this order. Third, the architecture is constructed hierarchically on length scales from the nanometer to millimeter level. Fourth, the expressed form evolves not only over long periods of time but in some cases over individual lifespans (metamorphosis). These features suggest that the formation of complex form is connected with patterning processes which arise from dynamic interactions and information transfer present within multicomponent systems, rather than intrinsic structural parameters. Nevertheless, without an understanding of the structural basis of morphology it is difficult to progress to a process-based description of form. For this reason, we now discuss the classical approaches used to describe the equilibrium form and habit modification of inorganic crystals.

3. Growth and Form of Crystals

The geometric shape (habit) of a crystal is determined by the external expression of a selected set of symmetry-related faces. Although the unit cell symmetry governs the spatial relations between the faces, their selection is mechanistically determined by the relative rates of growth along different crystallographic directions. In general, faces perpendicular to the fast directions of growth have smaller surface areas and slow growing faces therefore dominate the morphology. A needle-shaped crystal therefore corresponds to fast growth along one specific axis, whereas preferential growth along two directions produces a platelike morphology. In each case, the relative rates of growth reflect differences in the interplay between the internal lattice structure and external environment of the crystallization system.

3.1. Equilibrium Morphology

Under equilibrium conditions, the morphology of a crystal is determined solely by intrinsic factors. The faces comprising the crystal habit correspond directly with the most energetically stable atomic planes in the lattice. These planes have low Miller indices (*hkl*) so they usually correspond to the symmetry of the Bravais lattice and the crystal shape is a macroscopic expression of the unit cell (Figure 2). Low index

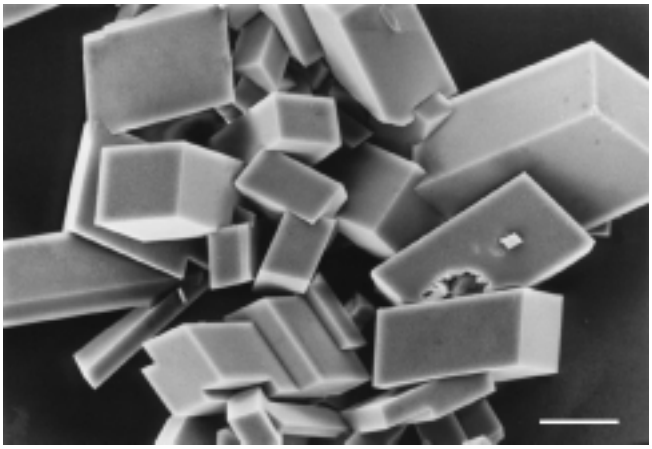

Figure 2. Scanning electron microscopy (SEM) image illustrating the correspondence between space symmetry and morphological form for calcite ($CaCO_3$) crystals grown under equilibrium conditions. The rhombohedral shape consists of six {10.4} faces and is a macroscopic expression of the $R\bar{3}c$ space symmetry of the unit cell. Scale bar = 10 μm.

faces are often relatively stable because they contain densely packed arrays of strongly bonded atoms. However, this simple structural approach does not always apply and a more complete description, involving knowledge of the surface energies ($\sigma_{s(hkl)}$) for all the crystal planes is required, where $\sigma_{s(hkl)}$ is defined as the excess energy per unit area of the surface lattice layer compared with the same plane in the bulk lattice. If the values for these energies can be obtained, either experimentally or from calculations, then the equilibrium crystal morphology possesses the Gibbs' condition for mimimum total surface energy for a given volume [Eq. (1)],[7] where $A_{(hkl)}$ is the surface area of the (*hkl*) crystallographic face.

$$\sum_{hkl} \sigma_{s(hkl)} A_{(hkl)} = \text{minimum} \quad (1)$$

Wulff proposed in 1901[8] that the shape of a crystal can be defined by vectors of length $l_{(hkl)}$, each of which is drawn

normal to the corresponding (*hkl*) face. Thus, according to the Gibbs' condition for minimum surface energy, these vectors have a length that is directly proportional to $\sigma_{s(hkl)}$. So if the surface energies of various planes are known then it is relatively simple to use a computer program to draw out the morphology from a set of vectors of known lengths and angular intercepts.

On this basis, there are several methods available for predicting the equilibrium form. Because a full treatment requires knowledge of the surface structure and a detailed description of the bonding between atoms in the surface layers and bulk lattice, the models have until recently been semiquantitative. Significant progress has been made by considering the number and types of periodic bond chains that exist in the plane of different crystal faces.[9] This relates to a value called the "attachment energy" which is the energy per molecule released when one slice of thickness $d_{(hkl)}$ is added onto the existing crystal face. If this value is low then the out-of-plane bonding is weak and the face is relatively stable because of the significant number of in-plane bond chains.

More recently, an atomistic simulation approach has been developed to predict inorganic crystal morphology.[10] For this, one needs to have a detailed understanding of the force field that describes the bonding in the crystal structure. In practice this means that the calculation of the lattice energy has to take into account not only the Born–Mayer electrostatic interactions between all the ions but the second-order short-range repulsive and attractive forces described by the Buckingham potential. Terms for bending and torsional potentials may also be required. To test the validity of the model and the corresponding interatomic potentials, calculations of the lattice energy and elastic constants are made and checked against reputable experimental values. Then the surface energies can be calculated by theoretically cleaving the crystal structure along a specific direction and allowing atoms on the new (*hkl*) surfaces to relax until they achieve a minimum energy configuration. The energy for the surface lattice is then calculated by using the interatomic potentials derived for the bulk lattice along with the structural details obtained by energy minimization. The surface excess energy is then given by the difference between the values calculated for the surface and bulk lattice structures.

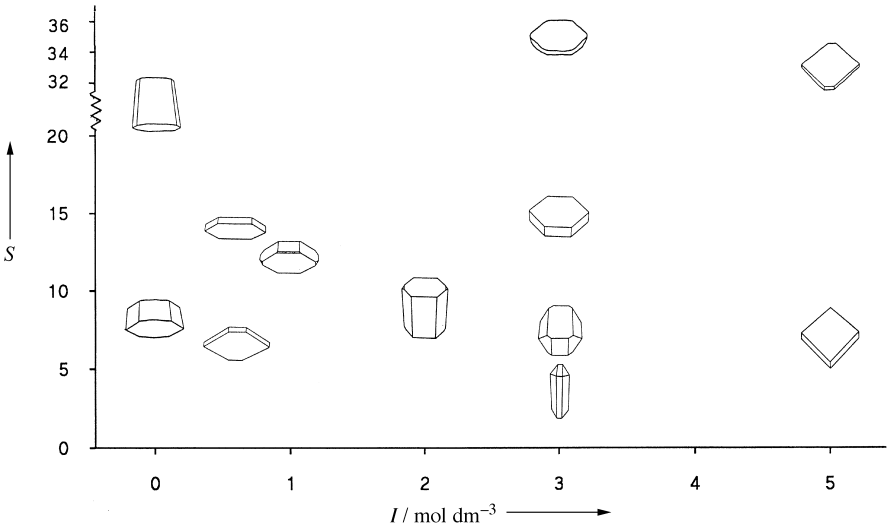

Figure 3. Plot of the morphological forms for $BaSO_4$ crystals grown under different conditions of supersaturation (S) and ionic strength (I). The crystals are drawn with their unit cell axes oriented in the same direction (the [001] axis is projected out of the page).[11]

3.2. Habit Modification

In practice, most inorganic crystals grow under nonequilibrium conditions and habits are strongly influenced by changes in supersaturation and ionic strength (Figure 3).[11] This raises the important question whether the rate of growth of a face is directly related to its intrinsic surface energy under nonequilibrium conditions, or arises as a consequence of mechanistic processes and interactions with the external environment. It seems reasonable that the rate of growth of a face that is relatively stable (low surface energy) will be mechanistically slow. Moreover, because different crystal faces have different surface energies, the relative rates of growth should be proportional to the energy differences provided that the growth mechanism is the same on each face. Under these conditions, faces with high surface energies grow fast and become eliminated in the final morphology.

The relative order of crystal surface energies, as well as the mechanistic processes of growth, can be dramatically changed by the preferential adsorption of soluble additives to specific faces. Systematic modifications in morphology can occur. For example, the rhomohedral habit of calcite ($CaCO_3$) crystals shown above in Figure 2 changes to a tabular form in the presence of Li^+ ions (Figure 4), which adsorb specifically on to

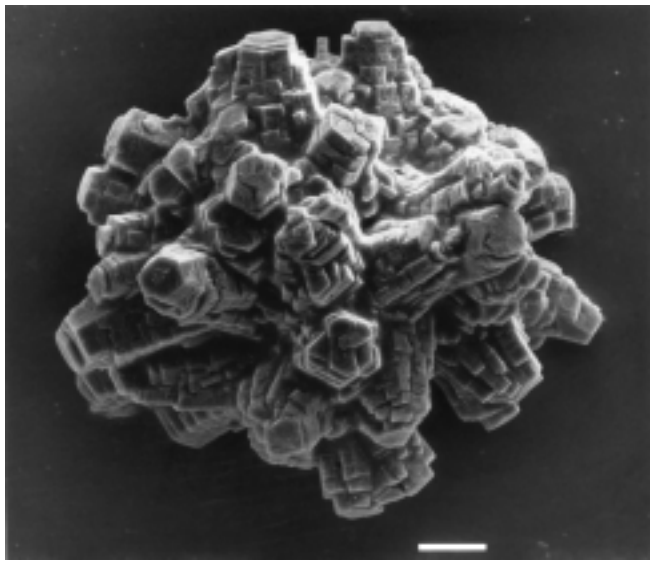

Figure 4. SEM image of a polycrystalline aggregate of calcite grown from supersaturated calcium bicarbonate solution in the presence of Li^+ ions. The tabular outgrowths originate from the preferential interaction of the additive with the {001} faces that lie perpendicular to the crystallographic c axis. Scale bar = 10 μm.

the {001} planes and inhibit growth of these faces.[12] It is generally true (but not always) that the crystal face perpendicular to the direction of growth that is inhibited by the additive increases in surface area. This means that it is often easy to read out from the changes in the relative areas of the faces in the modified morphology which crystallographic planes specifically interact with the soluble additive.

If the rate of crystal growth can be equated with the surface energies of particular crystal faces then it should be possible to accommodate the thermodynamic principles described above within a kinetic approach to crystal morphology. We would then be able to calculate the relative changes in surface energies of particular faces resulting from their interactions with additive molecules and predict the resulting habit modifications. For example, the surface energies for various calcite crystal faces with 50 to 100% coverage of Mg^{2+}, Li^{+}, or HPO_4^{2-} ions have been calculated and the resulting morphologies predicted are in agreement with calcite crystallization experiments.[10] The results predict the rhombohedral equilibrium form and show how it is modified by preferential lowering of certain faces ($\{1\bar{1}.0\}$ for Mg^{2+} and HPO_4^{2-}, {001} surface for Li^{+}) to produce crystals with prismatic or tabular habits (Figure 5).

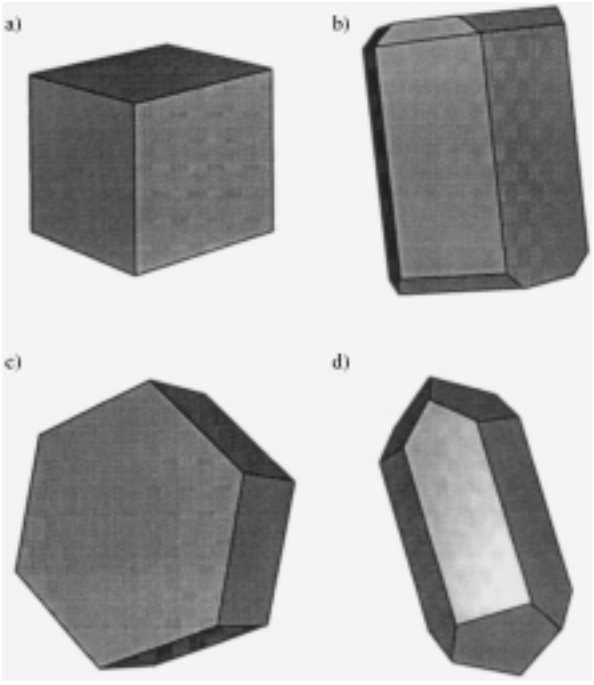

Figure 5. Predicted morphologies based on atomistic simulation of calcite surfaces in the presence of various additives. a) {10.4} rhombohedral (no additives), b) $\{1\bar{1}.0\}$ prismatic, stabilized by Mg^{2+}, c) {001} tabular, stabilized with Li^{+}, d) prismatic-rhomb $\{1\bar{1}.0\}/\{10.4\}$, stabilized with HPO_4^{2-}.

How successful this approach will be as a general method for predicting habit modification awaits further research. Besides the intrinsic problems of determining accurate interatomic potentials that can realistically describe the force fields of the modified inorganic surfaces, there are major reservations about the absence of mechanistic features—kinks, steps, screw dislocations etc—that underpin the kinetic theories of crystal growth. It seems clear from atomic force microscopy (AFM) studies that morphological changes can accompany the preferential interaction of additives with step and kink sites present on low-energy surfaces that changes the growth kinetics along certain directions.[13] Even though these mechanistic effects result in changes in the localized surface energies, they are too transient to be described by an atomistic simulation model which considers only equilibrium states on modified surfaces.

One central problem of the kinetic description of morphology is that the kink/step sites are treated as abstract geometric entities in theories of inorganic crystal growth. In reality, these sites have a molecular structure and shape derived from a localized perturbation in the relaxed surface lattice. If we could model the structure and dynamics of these sites then we might be able to simulate how they interact electronically and stereochemically with particular additive molecules. It is conceivable that these crystal surface interactions exhibit levels of molecular recognition analogous to biochemical processes such as antibody–antigen, and enzyme–substrate binding.

3.3. Molecular Recognition

Although no high-resolution structural details are currently available, there is circumstantial evidence that strongly suggests that molecular recognition in the form of charge, stereochemical, and structural matching of anion binding with packing motifs in crystal surfaces is an important factor in controlling the habit modification of inorganic crystals. The specificity of the interactions between additive and crystal surface growth sites are concentration dependent and can be dramatically changed through small modifications in the molecular structure of the soluble molecule.

Low molecular weight additives that have molecular structures with variable conformational states interact with inorganic crystal surfaces principally through electrostatic and stereochemical processes. For example, α-ω-dicarboxylic acids $[(CH_2)_n(CO_2H)_2]$ are effective at stabilizing faces essentially parallel to the $\{1\bar{1}.0\}$ surface of calcite provided that both carboxylate groups are ionized and $n < 3$ (Figure 6).[14] These faces contain both Ca^{2+} and CO_3^{2-} ions with the latter oriented such that the plane of the triangular anion is perpendicular to the surface. Thus incorporation of carbonate anions into the $\{1\bar{1}.0\}$ face during growth occurs through bidentate binding of two of the three oxygen atoms to Ca^{2+} ions in the surface. This stereochemical arrangement can also be adopted by binding of the dicarboxylate to the crystal surface (Figure 7). Moreover, both carboxylates in the additive molecule can bind simultaneously to two different calcium ions if the spacing between the CO_2^{-} groups is close to 0.4 nm. Both malonate ($n = 1$) and the unsaturated diacid, maleate (*cis*-$^{-}O_2CCH{=}CHCO_2^{-}$) fit this criterion but the increased rigidity of the latter reduces the binding affinity. The *trans* isomer, fumarate, has no morphological effect because cooperative binding can not take place.

It is important to note that the potency and morphological specificity of these dicarboxylate additives are lost at high concentrations where nonspecific binding becomes para-

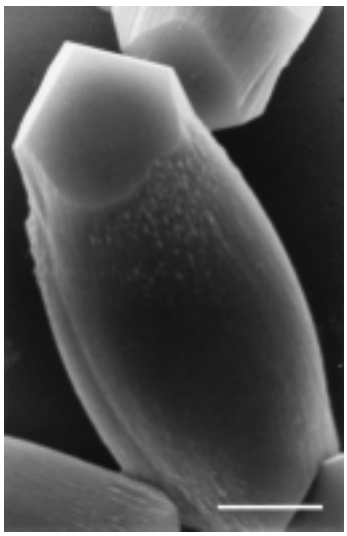

Figure 6. SEM micrograph of a spindle-shaped calcite crystal grown from supersaturated calcium bicarbonate solution in the presence of malonate at $[Ca^{2+}]$:[malonate] = 3.16. Crystal faces approximately parallel to the *c* axis are severely inhibited by the additive. Scale bar = 5 μm.

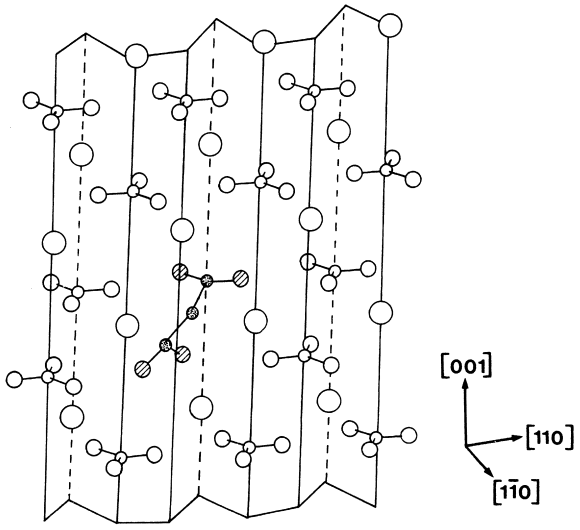

Figure 7. Perspective drawing of the calcite {1$\bar{1}$.0} face showing a possible binding site for malonate anion.

mount. On the other hand, they can be increased by additional charge functionalization in the molecule. For example, both α-aminosuccinate (aspartate) and γ-carboxyglutamate show more effective stabilization of the prismatic calcite {1$\bar{1}$.0} faces than succinate or glutamate.[14]

There are also a growing number of examples where macromolecular additives can have specific effects on crystal habit. For example, polysaccharides such as sodium alginate and various carragheenans, when added to supersaturated solutions of sodium chloride, inhibit surface nucleation by adsorption onto edge sites allowing dislocation growth to dominate over edge nucleation.[15] The resulting crystals have a well-defined cubic habit compared with the control crystals prepared in the absence of the inhibitors. Clearly, when one begins to consider the stereochemical possibilities of macromolecular interactions with inorganic crystal faces, then the recognition processes can become extremely complex and subtle. Studies have shown that acidic macromolecules extracted from the Mg-calcite biominerals of adult sea urchins interact specifically with calcite prismatic faces lying almost parallel to the {1$\bar{1}$.0} surface.[16] These molecules have high levels of aspartic and glutamic acid residues that can stereochemically mimic the coordination environment of ions in the {1$\bar{1}$.0} face by bidentate binding to the surface growth sites.

Understanding the molecular-specific interactions between surface-active molecules and selected crystal faces offers the potential to design additives for specific morphological changes. This has been achieved for example through the molecular synthesis of certain diphosphonate additives that interact specifically with $BaSO_4$ crystals grown from aqueous solution.[17]

4. Growth and Form of Biominerals

The majority of biominerals, such as bones, shells, and teeth, have complex morphologies that bear little resemblance to the same minerals formed in chemical or geological systems (Figure 1). Indeed, the shape of biominerals challenges the structural view of morphology presented above because there appears to be no direct relationship between the unit cell and the macroscopic form. Thus, ideas about the systematic habit modification of equilibrium shapes offer little help in explaining the complex spiral forms of calcium carbonate seashells or lacelike porous silica skeletons of diatoms. However, an understanding of biomineral morphogenesis might provide new concepts and insights for the chemical synthesis of complex form.

As a general principle, we can consider biomineralized structures to originate from the vectorial regulation of crystal growth and patterning in or between organic assemblies such as vesicles and polymeric frameworks.[18] The elaborate inorganic shapes arise from replication of the associated organic matrix through processes that are analogous to a cast produced in a mould. Metaphorically, the process of biomineralization acts as a "chemical medusa" that transforms soft organized matter into hard stonelike structures. In some systems, inorganic deposition and vesicle shaping proceed in concert, with the mineralization front remaining some distance behind the developing organic structure. Under these circumstances, synergistic interactions between the mineral and vesicle induce changes in the patterning process through coupling of the inorganic and organic processes. In particular, as the mineral begins to dominate the replicated organic morphology and the shape rigidifies, there is no longer any requirement for the vesicle to be held in place by associated biological structures, such as microtubules, and the patterning process becomes modified.

The general features of pattern formation in biomineralization[19] are illustrated in Figure 8 in which the dynamic shaping of vesicles takes place by anchoring the lipid membrane through the use of microtubule-based directing agents to an underlying scaffold like the cell wall. Intracellular space is criss-crossed with microskeletal networks and associated stress fields, so the equilibrium spherical shape of a

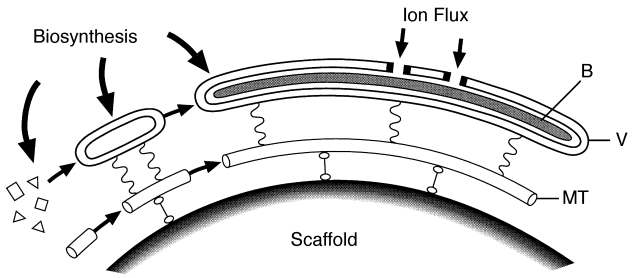

Figure 8. Illustration of the general features of programmed assembly in biomineralization. Cell walls, intracellular organelles and cellular assemblages can act as scaffolds for the assembly of microtubules (MT) which in turn are used as directing agents for the patterning of vesicles (V) involved in biomineralization (B).

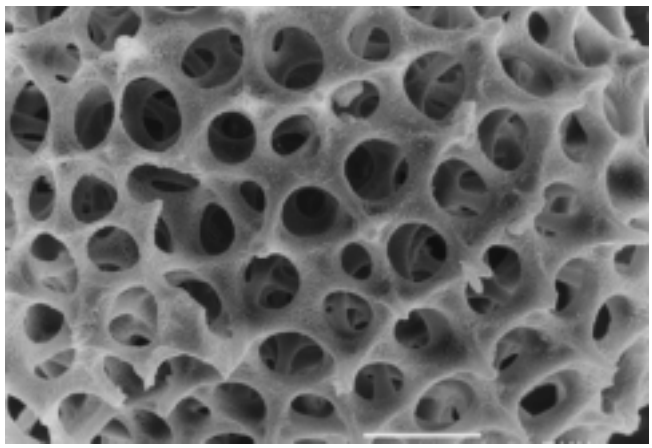

Figure 9. High-magnification SEM image of a radiolarian shell showing the void space patterning and continuous silica wall structure formed by mineralization in an organized "vesicle foam". Scale bar = 10 μm.

vesicle membrane can be readily distorted by mechanical and structural forces operating locally and at a distance. Empirically, it appears that the shaping of a vesicle can be directed by two perturbing force fields acting either tangentially along the surface of the cell wall or an internal organelle (for example the endoplasmic reticulum and nuclear envelope), or radially along structural filaments such as those based on the protein, tubulin. Very complex morphologies are produced if the radial and tangential growth of vesicles and their associated biominerals are coupled in a programmed sequence. For example, many radiolarian microskeletons exhibit several concentric shells of reticulated silica that are structurally connected by radiating arrays of small silica spicules.[20]

Assemblies of close-packed vesicles are used as patterning templates for the construction of the porous silica shells of radiolarians and diatoms (Figure 9). The complexity of the shell (frustule) can be rationalized on the basis of geometric packing of large "areolar" vesicles (AV) that are secreted and attached to the membrane wall (plasmalemma, PL) of the cell prior to mineralization (Figure 10). The vesicles are arranged into a thin polygonal foam with organized interstitial spaces that become mineralized in the form of a continuous silica framework. The vesicles remain unmineralized and are therefore used to pattern the void spaces in the silica skeleton. Thus, the diversity of patterns observed in diatom shells can be explained by geometrical deviations in the close packing of the areolar vesicles against the curved cell surface. However, this is not controlled primarily by surface tension but is the consequence of programmed cellular organization within the interstitial spaces that results in the secretion and assembly of tubular vesicles and associated microtubules in the gaps between the large areolar vesicles (Figure 10).[21] Silica deposition is confined tangentially to the tubular system such that an open geometric mesh of mesopores is established. The areolar vesicles subsequently detach and withdraw from the plasmalemma, and the resulting space is infiltrated with smaller vesicles that produce a thin patterned shell of silica across the top of the void spaces.

The sculpting of biomineral form represents a compromise between the force fields of inorganic crystallization and biological organization. In some systems, the intrinsic crystallographic anisotropy of a mineral such as calcite ($CaCO_3$) is exploited in the biomineralization of elongated spicules by aligning the direction of fast crystal growth (*c* axis) with the morphological long axis defined by the underlying stress filaments of the vesicle system. In others, the genetic patterning of vesicle morphogenesis offsets the intrinsic crystallographic symmetry to produce complex shapes (e.g. coccoliths) that bear no resemblance to the underlying crystal structure. In both cases, the high fidelity of mineral replication arises from patterning processes that are ultimately programmed by genetic information. However, on close inspection it becomes clear that even between individual organisms of the same species, the complex biomineral forms are similar but not identical. That is, they are reproducibly recognizable but not perfect copies. This morphological similarity (equiva-

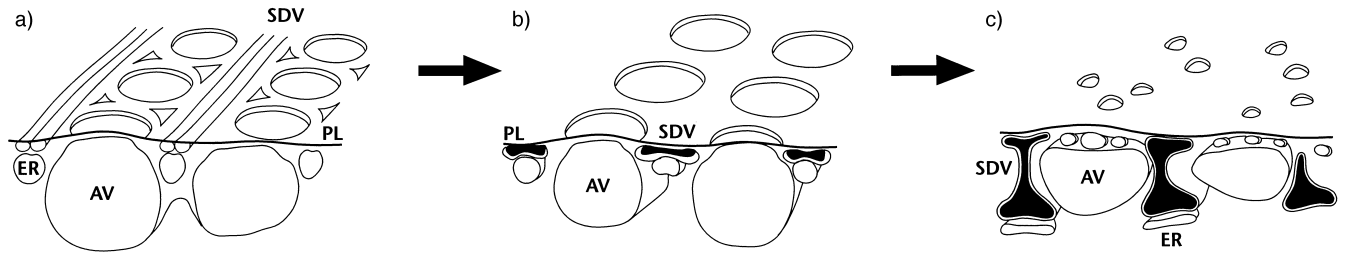

Figure 10. Illustration of the key stages in the formation of the siliceous diatom exoskeleton. a) Silica deposition vesicles (SDV) are preorganized with microtubules around the boundary spaces of large areolar vesicles (AR) attached to the plasmalemma (PL). b) The SDVs are mineralized with amorphous silica to give a patterned porous wall. c) The mineralized wall is thickened by extension of each SDV in association with the endoplasmic reticulum (ER). In some diatoms, detachment and retraction of the areolar vesicles from the plasmalemma results in infiltration with new SDVs and further mineralization of the pore spaces. Adapted from reference [21].

lence) reflects the tension between predetermined genetic mechanisms involved with the formation of the organic matrix, and the indeterminacy of fluctuations in the surrounding chemical and physical environment during the lifetime of the organism. Biomineral assembly is therefore determined by the complex interplay between the chemistry and geometry of the biological environment, both of which vary with time.

5. Morphosynthesis of Biomimetic Form

The vectorial regulation of the shaping and patterning of vesicles associated with the morphogenesis of biominerals such as coccoliths and diatom shells is inspiring new synthetic approaches to inorganic materials with complex form. The aim of *morphosynthesis* is to prepare inorganic materials with biomimetic form by direct chemical routes.[19, 22] In this section we highlight how the coupling of inorganic mineralization and instability thresholds in the surrounding reaction environment is a central feature of morphosynthesis. For example, complex inorganic morphologies can be produced by fluctuations in chemical processes that cause local perturbations in the stability of fluid–solid interfaces during mineralization. Similarly, the confinement of inorganic deposition within organized reaction environments (reaction fields) formed from compartmentalized fluids, such as microemulsions and biliquid foams, can result in complex forms, particularly when the reaction fields become unstable by in situ mineralization. And in the special case of mineral–surfactant mesostructures, structural modulations during growth can lead to curved forms through the interplay of bending, twisting, and compaction forces.

We now discuss some of the main chemical principles of morphosynthesis. A summary of the various approaches and typical materials produced is given in Table 1.

5.1. Fluid–Solid Instabilities

The fluid–solid interface of a growing crystal is susceptible to extrinsic factors that induce local instabilities and produce complex shapes and patterns. For example, unusual inorganic morphologies can be prepared from crystallization reactions in viscous solutions or gels in which nonlinear processes arising from chaotic mixing, vortex formation, diffusion and chemical gradients, and instabilities in hydrodynamic flow give rise to spatial and temporal patterns in mineral deposition at the fluid–solid interface. Banded inorganic structures (Liesegang's rings) are observed in silica and agar gels, and calcium phosphate precipitation in collagen gels gives rise to branched fractal structures.[23] In most cases, the periodicity and patterning of precipitation arises from diffusion-limited and mass transport processes in the fluid, and can be mathematically modeled.[24]

More complex inorganic forms are produced if the chemical reactivity of a viscous phase such as a silica gel is increased. For example, helical ribbons and spiral foils of calcium carbonate are obtained when solutions containing Ca^{2+} or HCO_3^- ions are allowed to counter-diffuse through a silica gel raised to pH values above 8.[25] These shapes are the result of the interplay between localized growth and inhibition at the fluid–solid interface which arises from the indeterminate formation and rupture of a semi-impermeable calcium silicate membrane around the developing crystals—a phenomenon commonly observed in "crystal gardens". A similar mechanism is responsible for the formation of distorted spirals of calcium carbonate (vaterite) in aqueous solutions of polyaspartate.[26] Similar experiments with polyacrylate induce the formation of elaborate cone-shaped assemblies of $BaSO_4$ filamentous crystals that are hierarchically organized into complex architectures (Figure 11).[11]

The ability of soluble polymers to induce complex shapes in inorganic materials may be widespread and deserves further investigation. Usually, the main problem concerns finding the appropriate window of activity, which often corresponds to a very limited set of reaction conditions among many permutations (ionic concentrations, molar ratios, polymer molecular weights etc). However, when appropriate conditions are found, wonderful structures can arise from this purely empirical approach.

5.2. Reaction Field Replication

The simplest synthetic representation of a typical membrane vesicle used in biomineral morphogenesis is a supersaturated microemulsion water droplet stabilized in oil by the segregation of surfactant molecules, such as sodium dodecylsulfate, at the oil–water interface. These droplets can be used to prepare hollow mineralized shells by specific nucleation and growth of the inorganic phase at the surfactant head-

Table 1. Current strategies in morphosynthesis.

Strategy	Product	Systems	Materials
fluid–solid patterning	banded aggregates, helicoids	SiO_2/OH^- gel	$CaCO_3$
	filaments, cones	polyacrylate	$BaSO_4$
	banded shells	hydroxyethyl cellulose	$CaCO_3$
	spirals, helicoids	polyaspartate	$CaCO_3$
reaction field replication	hollow microshells	emulsion droplets	$CaCO_3$
	cellular thin films, porous microshells	microemulsion foams + latex beads	$CaCO_3$, Fe oxides, MnOOH
adaptive construction	microskeletal frameworks	bicontinuous microemulsions	$Ca_{10}(OH)_2(PO_4)_6$ SiO_2
	mesoskeletons, nested filaments	block copolymer micelles	Ca phosphate
structural modulation	twisted ribbons/cones helicoids	reverse micelles/ microemulsions	$BaSO_4$, $BaCrO_4$
	discoids, gyroids, helicoids	surfactant–silicate liquid crystals	mesostructured SiO_2

Figure 11. Hierarchical structure of $BaSO_4$ cones formed in the presence of a 0.5 mM aqueous solution of polyacrylate ($M_r = 5100$). The hollow cone consists of myriad smaller $BaSO_4$ cones that assembly from the close packing of nanofilaments. Scale bar = 1 μm.

groups. Moreover, if the droplets are stable during inorganic precipitation, the shell diameter can be controlled through adjustments in the amount of water in the microemulsion. For example, microemulsions containing micrometre-sized water droplets prepared from a supersaturated calcium bicarbonate solution have been used to prepare calcium carbonate (vaterite) hollow microsponges (Figure 12).[27] The droplets only become supersaturated when CO_2 is degassed from the solution. This occurs by nucleation of microbubbles of CO_2 at the oil–water interface of each droplet so that the vaterite crystals in the shell structure are "patterned" by the entrapped gas bubbles. Thus, each droplet becomes preserved in the form of a micrometer-size vaterite hollow spheroid with an unusual surface texture consisting of pores and indentations, 0.3 to 1 μm in size.

This strategy can be extended to the synthesis of inorganic materials exhibiting three-dimensional (3D) micrometer-scale frameworks if we reverse the phase structure to produce a biliquid foam consisting of high concentrations of oil droplets stabilized by a thin soapy aqueous film and a continuous phase of a supersaturated solution. The organized structure can be used as a biomimetic representation of the patterning of the silica shell of diatoms by the space-filling aerolar vesicles that we discussed previously. For example, stabilized foams of freon (fluorotrichloromethane) droplets dispersed in water have been used to prepare honeycomb silica morphologies by in situ gelation of a silica sol within the boundary and interstitial spaces of the organized fluid.[28]

Another strategy is to produce transitory foams by spreading a thin film of a supersaturated microemulsion onto a metal substrate and partially removing the oil phase by washing with hot hexane. This destabilizes the microemulsion film and causes microphase separation of the remaining oil and supersaturated aqueous solution into a self-organized foam-like array of submicrometer-size oil droplets surrounded by supersaturated aqueous fluid. Growth of inorganic crystals then occurs in the interstitial spaces and boundary edges between the oil droplets to produce a mineralized imprint of the cellular structure. This approach has been used to prepare disordered frameworks of calcium carbonate (aragonite) and transition metal oxides (FeOOH, MnOOH) (Figure 13).[29] Typically, the cellular films have continuous, branched mineral walls 20 to 100 nm in width, and enclosed cells of average size, 45 to 300 nm, depending on the size of the oil droplets, which in turn are controlled by the reaction conditions. Because the foam is a transitory structure, mineralization and oil droplet self-assembly must occur almost simultaneous if the interstitial spaces are to be filled with a continuous inorganic framework of calcium carbonate or metal oxide. This is achieved, respectively, by outgassing of CO_2 from or O_2 diffusion into the microemulsion. Both these processes are accelerated as the air–water interfacial area increases during foam formation, and give rise to rapid increases in supersaturation in the interstitial spaces by shifting the carbonate–bicarbonate and Fe^{II}/Fe^{III} redox/hydrolysis equilibria, respectively.

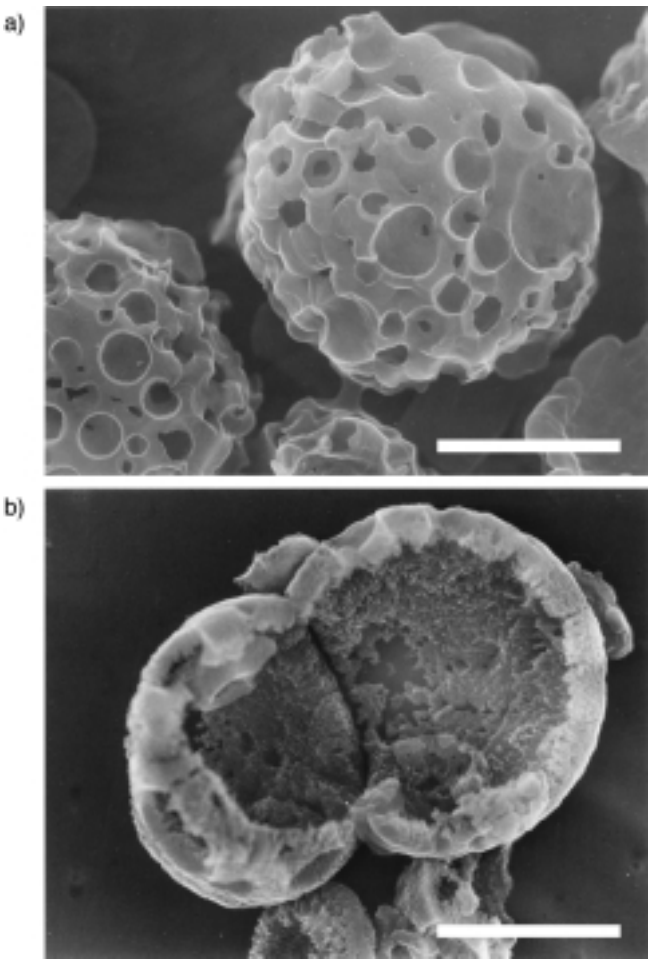

Figure 12. SEM images showing spongelike vaterite spheroids prepared from water-in-oil supersaturated microemulsions (octane:sodium dodecylsulfate:$CaHCO_3$ = 71:4:25 wt %). a) Individual vaterite spheroid showing complex surface patterning, b) broken spheroid showing hollow internal space. Scale bar = 10 μm, for both micrographs

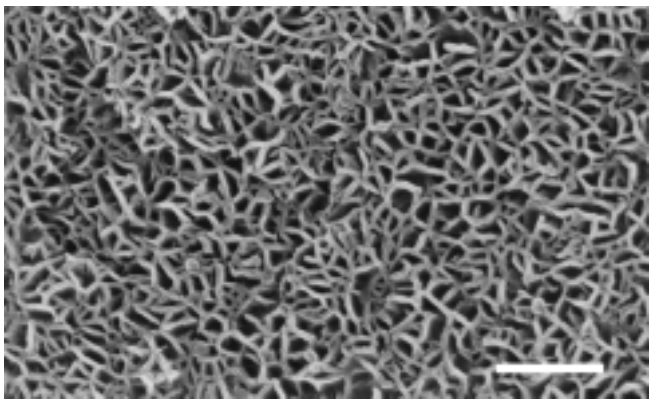

Figure 13. SEM image of a cellular film of $CaCO_3$ (aragonite) synthesized by reaction field replication in a transitory oil droplet biliquid foam. Scale bar = 1 μm.

Sculpting these cellular films into closed microshells produces structures that can be loosely described as biomimetic coccoliths (Figure 14).[29] This is achieved by spreading the microemulsion film over micrometer-sized polystyrene beads and washing in hot hexane. Hexane is a suitable solvent

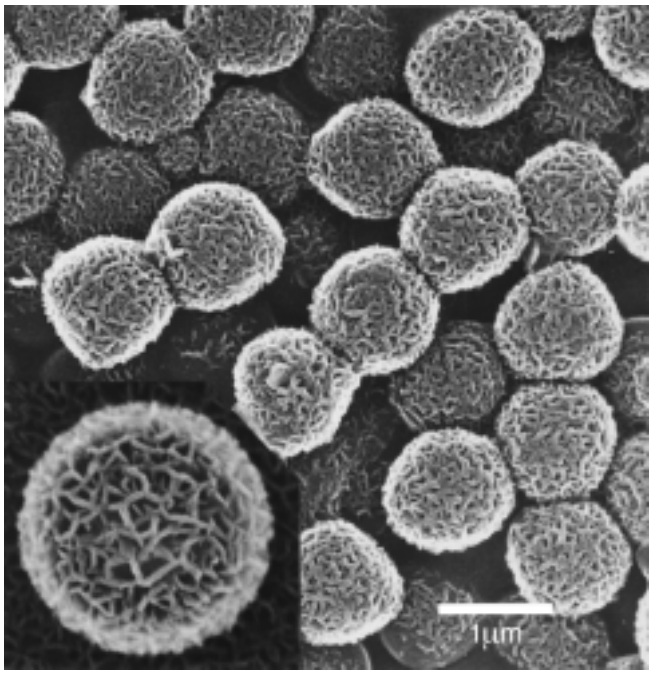

Figure 14. SEM image of intact hollow shells of mesoporous aragonite. Inset shows a high-magnification SEM image of an intact shell with well-defined cellular substructure. Scale bar = 1 μm.

because it does not dissolve the polymer template but induces demixing and mineralization of the transient cellular structure. The beads are then dissolved in chloroform or destroyed by heating to give porous hollow shells of cellular calcium carbonate or Fe oxide.

5.3. Adaptive Construction

The basic principle of reaction field materials replication rests on the assumption that there is a direct correspondence between the original shape and size of the fluid-filled environments and that of the final mineral phase. Clearly, in many cases this is not true because the development of the inorganic structure perturbs the local environment in which it grows. As the reaction field adjusts to the presence of the incipient mineral then this in turn influences the new growth directions and a feedback loop is established. Thus, the inorganic morphology becomes dependent on the interplay of these processs, their synergism, and how they change with time. Form is therefore an emergent property established by a process of adaptive construction.

An interesting aspect of these interactive systems is that the mineral morphology often superficially resembles the reaction field but is different when compared in terms of scale. For example, bicontinuous microemulsions assembled from mixtures of tetradecane, water and the cationic surfactant didodecyldimethylammonium bromide (DDAB) are structured as compartmentalized liquids in which the oil and water components are separated into highly branched and interconnected conduits, approximately 2 nm wide. By using a supersaturated calcium phosphate solution in place of water, and freezing the oil channels at temperatures above 0 °C, one might expect to replicate the reaction field as a nano-textured calcium phosphate phase. Instead, a remarkable microskeletal architecture, with micrometer-size pores in the interconnected framework, is deposited.[30] The scale is over two orders of magnitude greater in length than the channellike nanoscopic reaction environments. Similar micron-scale structures are obtained for silica polymerization in oil-frozen bicontinuous microemulsions.[31] In this case, the reaction proceeds by partitioning the alkoxide precursor, tetraethoxysilane (TEOS), in the oil channels and allowing the TEOS molecules to slowly hydrolyze at the oil–water interface. The silicate species then migrate into the water channels where they undergo condensation reactions to produce amorphous silica.

Analogous processes of adaptive construction are observed when the precipitation of calcium phosphate is carried out in soft colloidal aggregates formed from block copolymers consisting of a long poly(ethylene oxide) block and a short poly(methacrylic acid) domain that is partially alkylated with a long-chain amine group.[32] The polymer molecules are sufficiently hydrophobic that they self-assemble into 130 nm-size aggregates of entangled micelles to produce a colloid that is stable across a pH range of 3 to 9. Although the block-copolymer aggregates are polydisperse and disordered on the mesoscale, they are effective reaction fields for the sequestration of aqueous Ca^{2+}. At polymer to Ca^{2+} mole ratio of 4:1, nearly all the Ca^{2+} ions are associated with the acrylate and ethylene oxide groups so that the addition of phosphate ions at pH values between 3.5 and 5 increases the local supersaturation and results in the nucleation of calcium phosphate within the dispersed aggregates rather than in bulk solution. However, instead of the formation of small clusters of calcium phosphate embedded within the disordered polymer chains, a delicate mesoskeleton of interconnected inorganic needles evolves from the calcium-loaded aggregates. At pH = 3.5, the initial structures are 200 nm in size, with a starlike morphology consisting of a small number of 17 nm-thick inorganic filaments that are longer than the average diameter of the aggregate (130 nm) (Figure 15a). With time, the number of

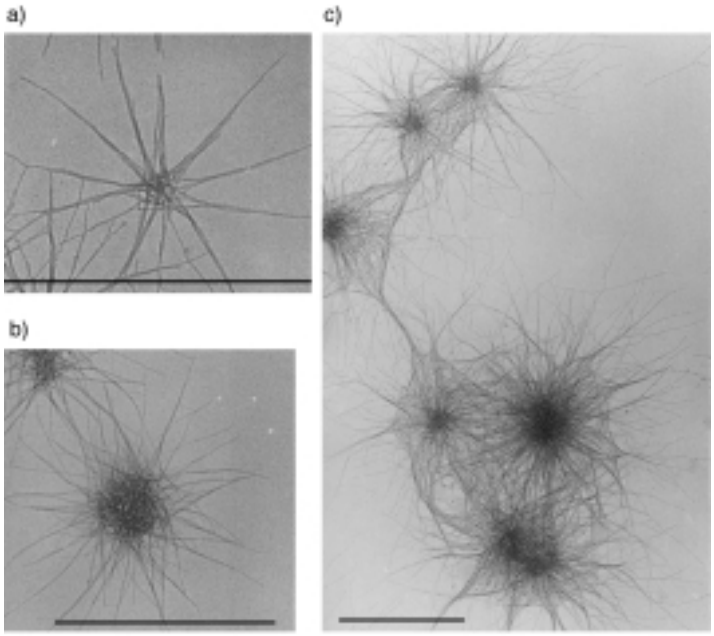

Figure 15. TEM images of calcium phosphate block copolymer nested colloids. a) Starlike form at early stage at pH 3.5, b) later stage showing complex central core, c) neuron-like tangles produced at pH 5. Scale bar = 0.5 μm.

filaments in each structure increases to produce a complex nested form (Figure 15b). After 100 h, the architecture becomes destabilized and the filaments reduce in length as the central core densifies to produce a mesostructured mineral-polymer colloid of similar diameter to the reaction field of the unmineralized aggregates. In contrast, the nested forms produced at pH 5 are stable and do not transform into the densified aggregate. Instead, the nanofilaments are thinner (3 nm) and longer (500 nm) than those initially formed at lower pH, and highly entangled to give neuron-like structures with a dense 120 nm-wide core (Figure 15c).

These complex forms represent higher-order coupling of the inorganic growth processes with changes in the organization and stability of the polymer aggregates. The concomitant changes in morphology represent adaptations to modifications in the structural, interfacial, and energetic properties of the coupled system. The supersaturation in the Ca^{2+}-loaded polymer aggregate is not particularly high at pH 3 because most of the phosphate anions are protonated. This means that interfacial factors, present solely within the reaction field of the polymer aggregate, promote the nucleation of calcium phosphate within these environments rather than in bulk solution. (At pH 7, no complex forms are observed because the rate of precipitation is fast due to the higher supersaturation and deposition in the bulk solution occurs). Once the inorganic clusters begin to grow within the colloidal aggregates competing force fields are set up as the particles push aside the entangled polymer chains. An instability threshold is reached when the polymer–mineral interactions become strong enough to disrupt the organic mesostructure and produce a cooperative growth process.

The exceedingly high anisotropy of the nanofilaments suggests that the polymer chains are strongly associated with all the inorganic surfaces except the tip, which is not blocked from further growth because these are the only sites exposed to phosphate anions diffusing from the bulk phase into the Ca^{2+}-loaded aggregates. In the early stages of growth only a few nucleation sites occur in the aggregates and these are propagated through and outside of the disordered polymer matrix to produce the delicate nanoskeletal forms. As the filaments extend beyond the aggregate, polymer molecules must be drawn out along the sides of the inorganic needles. This depletes the core of the aggregate, which reconstructs and becomes progressively unstable as the number of filaments increase. However, the metastability is maintained at pH 5 because the polymer-coated inorganic filaments, even though they are only 3 nm wide, are stable with respect to dissolution. In contrast, calcium phosphate is relatively soluble at pH 3 so the filaments start to dissolve as the supersaturation reduces with time. This allows the polymer aggregates to be reestablished along with a secondary calcium phosphate phase.

5.4. Structural Modulation

Morphological transitions similar to those described in the previous section are particularly prominent for ordered hybrid mesophases in which the inorganic and organic components are regularly arranged over distances of 3 to 5 nm. This arrangement is particularly susceptible to structural modulation because inefficient space-filling and mismatching in interfacial structure and charge readily lead to metastability and in situ changes in form. A similar process occurs for the calcium phosphate block copolymer nested colloids described above except that there is no intrinsic long-range ordering in the intermediate structures. When there is periodic ordering, local deviations in structure (density, defects) and surface energy (charge, hydrophobicity) can produce morphological curvature through processes of bending, folding, twisting, and elastic deformation. For example, such processes account for the growth and form of micrometer-long twisted bundles of $BaSO_4$ and $BaCrO_4$ nanofilaments in water-in-oil microemulsions prepared from the anionic surfactant, sodium bis(2-ethylhexyl)sulfosuccinate (commonly called, AOT) (Figure 16a).[33] The reaction occurs at room temperature in unstirred isooctane containing a mixture of $Ba(AOT)_2$ reverse micelles and NaAOT microemulsions with encapsulated sulfate (or chromate) anions. The reverse micelles are about 2 nm in diameter and consist of a spherical cluster of about 10 Ba^{2+} ions strongly associated with the sulfonic acid headgroups of the surfactant, along with water of hydration. In contrast, the microemulsions are larger (4.5 nm across) because they contain bulk water (aqueous Na_2SO_4 or Na_2CrO_4) at a water to surfactant molar ratio, $w = 10$. When mixed together, the two reaction fields interact so that the constituents are slowly exchanged and $BaSO_4$ or $BaCrO_4$ nanoparticles nucleate and grow within the delineated space.

Discrete nanoparticles, 11 nm in size, are only formed in this system if the anion concentration is two to five times that of the Ba^{2+} ions.[34] Under these conditions, the surface charge

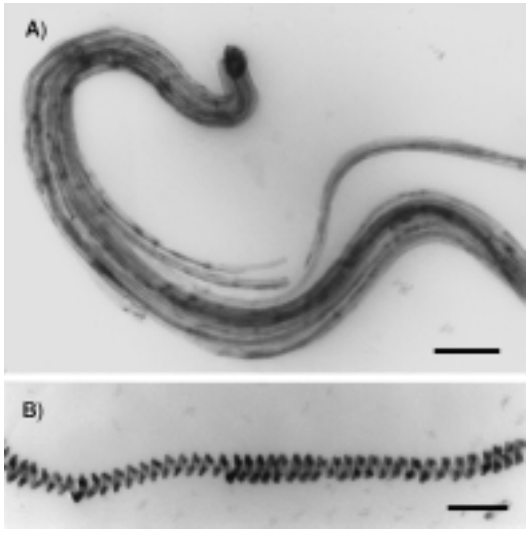

Figure 16. TEM images of $BaSO_4$ complex fibers showing; a) closely packed bundle of nanofilaments and coiled terminus, b) helical filament with 40 nm pitch. Scale bars = 200 nm.

on the $BaSO_4$ or $BaCrO_4$ crystals is negative (a surface excess of anions) and there is therefore minimal interaction with the anionic headgroups of the AOT molecules. On the other hand, if there is a stoichiometric excess of Ba^{2+} ions the nanoparticles are positively charged and the AOT molecules are strongly adsorbed onto the inorganic surfaces and growth is terminated by the time the clusters reach 5 nm in size. Furthermore, the pinning of the AOT molecules onto the surface induces aggregation of the clusters by inter-particle interdigitation of the immobilized surfactant chains. The clusters aggregate into a linear array that fuses together to give a single 5 nm-wide crystallographically aligned inorganic filament. The structural reconstruction originates from the strong coupling between the increase in inorganic lattice energy and reduction in membrane curvature that specifically accompanies linear association. Moreover, the structure propagates along one direction because surfactant molecules at the tips are readily displaced compared with those assembled along the filament edges.

With time, other filaments are formed parallel to the original thread to produce a small bundle of coaligned inorganic nanofilaments held together by surfactant bilayers. The locking in of new filaments by surfactant interdigitation generates a bending force in the nonattached segment of the longer primary thread. This results in the coiling of the bundle into a characteristic spiral-shaped structure several hundred nanometers in size that becomes self-terminating at one end because further addition of the primary nanoparticles is prevented by spatial closure. The final angle of rotation is dependent on the number of secondary nucleation events that occur on the internal edge of the primary filament. Since the number of coaligned filaments increases as the structures grow away from the terminus, the bending energy decreases and the bundle becomes straight. However, two further structural modulations can occur as the bundles extend in length. First, dissipation of strain energy arising from lateral packing pressure causes some bundles to splay outwards into cone-shaped growth ends. Second, if the strain energy is low and the bundle is relatively thin, then differences in rigidity along the bundle can induce twisting of the filaments. This can arise from the lateral fusion and compaction of filaments by displacement of the AOT bilayers, and takes place initially in the older coiled end of the bundle. Because the twisting is not associated with any stress field or elastic deformation, it can propagate throughout the length of the bundle as the filaments coalesce to produce a single-crystal helicoid (Figure 16b).

Similar explanations account for the remarkable morphologies observed for surfactant–silica hexagonal mesophases formed in quiescent acidic medium.[35] These materials consist of closely packed silica-coated rodlike micelles that can easily bend through 180° if the surface charge is not too high to produce topological defects that generate curved gyroids and discoids. Moreover, the low surface charge favors a growth model in which the curved micelles are added side-on to the existing structure. In contrast, a straight fiberlike morphology is produced under very acidic conditions because the highly protonated surfaces maintain a rigid-rod conformation that sustains an end-on growth mechanism.

The liquid crystalline nature of these mesophases makes them susceptible to elastic deformations that become manifest in regular radial patterns at the surface of the discoid form. Moreover, the polymerization of silica between the micelle rods is a slow process so that the initially formed regions, such as the center of the discoids, are more densely compacted than those at the edges. This differential contraction parallel and perpendicular to the rods leads to folding of strips of the structure into an open-ended microscopic helical tube. When the twisting is combined with differences in polymerization (contraction) along the tube, wonderful archimedean screwlike shapes are produced.[36]

6. Higher-Order Assembly

Many biominerals exhibit complex forms that arise from the organized assembly of preformed mineral building blocks. These structures are associated with a variety of constructional processes involving the cellular processing of shaped and patterned biominerals into higher-order assemblies with micro- or macroscopic architecture. For example, magnetite crystals in magnetotactic bacteria are sequentially synthesized along a linear chain of vesicles so that the cells contain a permanent magnetic dipole for navigation in the geomagnetic field.[37] In certain protozoa, curved silica rods are transported sideways through the cell membrane and out into the extraellular space, where they act as building blocks for the construction of an open-ended basketlike framework (lorica).[38]

These biomineralization processes are inspiring new ideas in *crystal tectonics*, which can be defined as the chemical construction of higher-order structures from solid-state building blocks, such as inorganic nanoparticles. To achieve this, there has to be sufficient informational content in the preformed inorganic surfaces to control long-range ordering through interactive self-assembly. A relatively simple level of

communication is achieved by the interdigitation of surfactant chains attached to nanoparticle surfaces. The hydrophobic driving force for assembly gives rise to a bilayer between adjacent particles and this becomes directional if the organic molecules are located on specific crystal faces. For example, we described above how it was possible to chemically synthesize complex filamentous structures by a process that involved surfactant-induced linear coalescence of $BaSO_4$ or $BaCrO_4$ nanoparticles. Clearly, by preventing the fusion of the nanoparticles whilst maintaining a degree of micellar aggregation, it should be possible to synthesize a linear array of discrete spatially separated inorganic crystals. This has been achieved by increasing the stability of the individual nanoparticles without compromising the aggregation process. These criteria are met when the surface charge of the crystals is close to neutral, that is when the $[Ba^{2+}]$:$[SO_4^{2-}]$ (or $[Ba^{2+}]$:$[CrO_4^{2-}]$) molar ratio is equal to 1.0. Under these conditions, remarkable linear chains of individual $BaSO_4$ or $BaCrO_4$ nanoparticles are formed in a single step from the microemulsion reaction media (Figure 17).[34] The colloidal

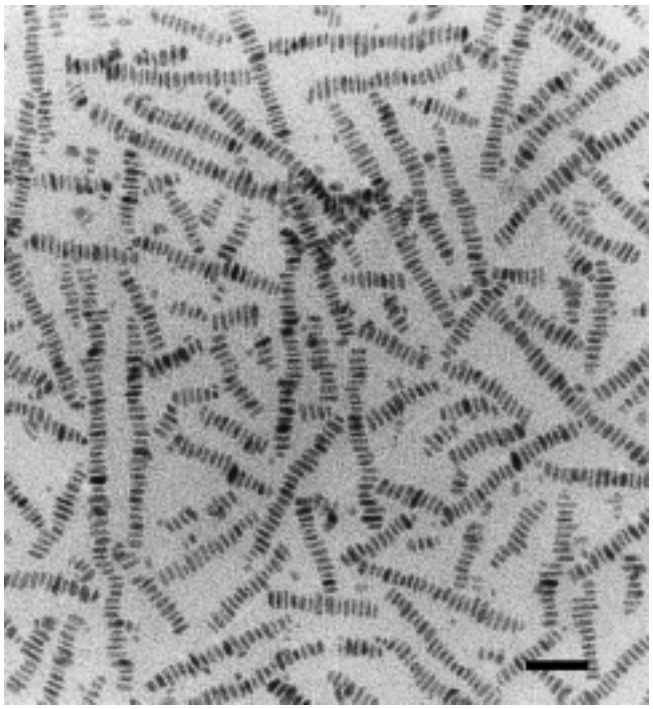

Figure 17. TEM image showing ordered chains of prismatic $BaSO_4$ nanoparticles prepared in AOT microemulsions at $[Ba^{2+}]$:$[SO_4^{2-}]$ molar ratio = 1 and $w = 10$. Scale bar = 50 nm.

chains are 50 to 500 nm in length and assembled directly in solution. Each chain consists of discrete rectangular prismatic crystals that are uniform in size ($16 \times 6.8 \times 6$ nm at $w = 10$) and preferentially aligned with the long axis of each particle perpendicular to the chain direction. Significantly, a regular spacing of 2 nm, corresponding to an interdigitated bilayer of surfactant molecules, separates each crystal in the chain so that they look like a biomimetic counterpart of the linear chains of discrete membrane-bounded magnetite chains synthesized in magnetotactic bacteria.[37]

The linear arrays spontaneously form in the microemulsion fluid so nanoparticle synthesis and self-assembly are intimately coupled. The ordered assembly is determined by the uniformity in particle size in combination with crystal faces of regular shape and size. Together these facilitate crystal face-specific interactions between the hydrophobic tails of AOT molecules adsorbed onto the flat side faces of the $BaSO_4$ or $BaCrO_4$ prismatic crystallites. This process occurs specifically along one direction because there are two sets of side faces that differ in surface area. Aggregation is therefore directed along the axis perpendicular to the larger faces because this maximises the hydrophobic – hydrophobic interactions between the crystals and lowers the free energy of the surfactant – nanoparticle biphase.

7. Summary and Outlook

Natural form is a spatio-temporal representation of chemical processes that are programmed by genetic information. The study of such processes, for example in biomineralization, should lead to similar emergent properties in chemical systems. As a first step towards the chemistry of form, this article has traced a route from the equilibrium form of crystals to the synthesis of complex shapes by reactions in organized fluids. In general, crystal morphology is determined by the relative rates of growth of different crystal faces, with the slow growing surfaces dominating the final form. The equilibrium shape therefore consists of the set of symmetry-related faces that give the minimum total surface energy, and can be predicted from knowledge of the surface structures and bonding interactions. Low and high molecular weight additives can stabilize nonequilibrium morphologies by changing the relative growth rates of different crystal faces through molecular-specific interactions with certain surfaces that modify the surface energy or growth mechanism, or both.

The vectorial regulation of the shaping and patterning of vesicles associated with the morphogenesis of biominerals such as coccoliths and diatom shells is inspiring new synthetic approaches to inorganic materials with complex form. The aim of morphosynthesis is to prepare inorganic materials with biomimetic form by direct chemical routes and central to this process is the coupling of inorganic precipitation and instability thresholds in the surrounding reaction environment. A number of systems have been discussed in this review. For example, the fluid – solid interface of a growing crystal is susceptible to extrinsic factors that induce local instabilities and produce complex shapes and patterns. And porous inorganic shells and membranes can be synthesized by materials replication of stable or transitory reaction fields established in microemulsion droplets and biliquid foams. Significantly, mineral-induced instabilities in channellike microemulsions and block-copolymer aggregates give rise to the emergence of complex three-dimensional inorganic morphologies through time-dependent correlations and adaptations. Curved morphologies are also produced in ordered inorganic – organic mesophases by structural modulations that give rise to bending, twisting, folding, and elastic deformation. Finally, nanoparticle synthesis and self-assembly can be

coupled by the interfacial activity of reverse micelles and microemulsions to produce higher-order forms such as linear chains.

In biology, the general features of form are clearly connected to function—bone shape to movement, for example. But the elaboration of fine structure may be redundant. For example, whilst it is important to pattern voids in the exoskeleton of a diatom for chemical communication with the external environment, the exact shape of the pores may be functionally irrelevant. Thus a wide range of species-specific pore shapes appear to have evolved from subtle changes in processing rather than functional advantage. This fluidity of form in function raises important issues for a chemical approach to morphology with technological exploitation as an immediate goal. It is well known that the shape and texture of materials determine properties such as the long-term stability of products, flow and transport behavior, catalytic activity, separation efficiency, and adhesion. Synthesizing inorganic materials with complex patterns will therefore be relevant to the design of new types of catalyst supports, membranes for the separation of large polymers, colloids and cells, biomedical implants with macroporosity, drug carriers, and vectors for delivery and release of viruses and DNA in transfection procedures. At the current time, however, we have few ideas about the level of precision required to match form to function in synthetic applications.

I am indebted to many scientists for their contributions to the work described in this review. In particular, I wish to express my thanks to; Professor Steve Parker and Dr. James Titloye (University of Bath, UK) who pioneered the atomistic simulation of calcite surfaces and habit modification; Dr. Jon Didymus for his insightful studies on the growth and form of calcite in the presence of dicarboxylic acids; Dr. Dominic Walsh for his pioneering contributions in the study of calcium carbonate and calcium phosphate crystallization in microemulsions; Dr. Jeremy Hopwood for his discovery of $BaSO_4$ filaments and helicoids from microemulsion-based reactions; and Mei Li for her remarkable breakthrough in the higher-order synthesis and self-assembly of $BaSO_4$ and $BaCrO_4$ nanoparticles. I am also greatly indebted to Professor Markus Antonietti and Dr. Christine Goeltner and Dr. Helmut Cölfen (Max-Planck-Institut für Kolloid- und Grenzflächenforschung, Golm, Germany) for their frontier research on calcium phosphate-block copolymer micelles, and the many insights, technical skills, and creative ideas that they have shared throughout a long-standing and most enjoyable collaboration.

Received: February 17, 1999 [A 398]

[1] A. L. Mackay, *Forma* **1999**, *14*, 11.
[2] D. W. Thompson, *On Growth and Form*, Cambridge University Press, Cambridge, **1942**.
[3] P. Ball, *The Self-made Tapestry: Pattern Formation in Nature*, Oxford University Press, Oxford, **1999**.
[4] A. L. Mackay, *Mater. Sci. Forum* **1994**, *150*, 1.
[5] A. L. Mackay, *Theochem*. **1995**, *336*, 293.
[6] M. M. Helmkamp, M. E. Davis, *Annu. Rev. Mater. Sci*. **1995**, *25*, 161.
[7] J. W. Gibbs, *Collected Works*, Longman, New York, **1928**.
[8] G. Wulff, *Z. Krist. Kristallgeom*. **1901**, 949.
[9] P. Hartmann, P. Bennema, *J. Cryst. Growth* **1980**, *49*, 145.
[10] J. O. Titiloye, S. C. Parker, D. J. Osguthorpe, S. Mann, *J. Chem. Soc. Chem. Commun*. **1991**, 1494; J. O. Titiloye, S. C. Parker, S. Mann, *J. Cryst. Growth* **1993**, *131*, 533.
[11] J. D. Hopwood, Ph.D. thesis, University of Bath, **1996**.
[12] S. Rajam, S. Mann, *J. Chem. Soc. Chem. Commun*. **1990**, 1789.
[13] A. J. Gratz, P. E. Hillner, *J. Cryst. Growth* **1993**, *129*, 789; P. M. Dove, M. F. Hochella, *Geochim. Cosmochim. Acta* **1993**, *57*, 705.
[14] S. Mann, J. M. Didymus, N. P. Sanderson, E. J. Aso-Samper, B. R. Heywood, *J. Chem. Soc. Faraday Trans. 1* **1990**, *86*, 1873.
[15] J. D. Birchall, R. J. Davey, *J. Cryst. Growth* **1981**, *54*, 323.
[16] A. Berman, L. Addadi, S. Weiner, *Nature* **1988**, *331*, 546.
[17] R. J. Davey, S. N. Black, L. A. Bromley, D. Cottier, B. Dobbs, J. E. Rout, *Nature* **1991**, *353*, 549.
[18] S. Mann, *J. Mater. Chem*. **1995**, *5*, 935.
[19] S. Mann, G. A. Ozin, *Nature* **1996**, *382*, 313; S. Mann, *J. Chem. Soc. Dalton Trans* **1997**, 3953.
[20] O. R. Anderson, *Biomineralization in Lower Plants and Animals*, *Vol. 30* (Eds.: B. S. C. Leadbeater, R. Riding), Oxford Univeristy Press, Oxford, **1986**, pp. 375–391 (Systematics Association).
[21] R. M. Crawford, A.-M. M. Schmid *Biomineralization in Lower Plants and Animals*, *Vol. 30* (Eds.: B. S. C. Leadbeater, R. Riding), Oxford Univeristy Press, Oxford, **1986**, pp. 290–314 (Systematics Association).
[22] S. Mann, S. L. Burkett, S. A. Davis, C. E. Fowler, N. H. Mendelson, S. D. Sims, D. Walsh, N. T. Whilton, *Chem. Mater.* **1997**, *9*, 2300; G. A. Ozin, *Acc. Chem. Res.* **1997**, *30*, 17.
[23] R. Kniep, S. Busch, *Angew. Chem.* **1996**, *108*, 2787; *Angew. Chem. Int. Ed. Engl.* **1996**, *35*, 2624.
[24] H. K. Henisch, J. M. Garcia-Ruiz, *J. Cryst. Growth* **1986**, *75*, 195.
[25] J. M. Garcia-Ruiz, *J. Cryst. Growth* **1985**, *73*, 251.
[26] S. D. Sims, J. M. Didymus, S. Mann, *J. Chem. Soc. Chem. Commun.* **1995**, 1031; L. A. Gower, D. A. Tirrell, *J. Cryst. Growth*, **1998**, *191*, 153.
[27] D. Walsh, B. Lebeau B, S. Mann, *Adv. Mater.* **1999**, *11*, 324.
[28] M. Wu, T. Fujiu, G. L. Messing, *J. Non-Cryst. Solids* **1990**, *121*, 407.
[29] D. Walsh, S. Mann, *Nature* **1995**, *377*, 320; D. Walsh, S. Mann, *Adv. Mater.* **1997**, *9*, 658.
[30] D. Walsh, J. D. Hopwood, S. Mann, *Science* **1994**, *264*, 1576; D. Walsh, S. Mann, *Chem. Mater.* **1996**, *8*, 1944.
[31] S. D. Sims, D. Walsh, S. Mann, *Adv. Mater.* **1998**, *10*, 151.
[32] M. Antonietti, M. Breulmann, C. G. Goltner, H. Cölfen, K. K. W. Wong, D. Walsh, S. Mann, *Chem. Eur. J.* **1998**, *4*, 2491.
[33] J. D. Hopwood, S. Mann, *Chem. Mater*. **1997**, *9*, 1819; M. Li, S. Mann, *Langmuir* **2000**, *16*, 7088.
[34] M. Li, H. Schnablegger, S. Mann, *Nature* **1999**, *402*, 393.
[35] S. Oliver, A. Kuperman, N. Coombs, A. Lough, G. A. Ozin, *Nature* **1995**, *378*, 47; G. A. Ozin, *Can. J. Chem.* **1999**, *77*, 2001.
[36] S. M. Yang, I. Sokolov, N. Combs, C. T. Kresge, G. A. Ozin, *Adv. Mater.* **1999**, *11*, 1427.
[37] S. Mann, N. H. C. Sparks, R. G. Board, *Adv. Microbial. Phys.* **1990**, *31*, 125.
[38] B. S. C. Leadbeater, *Proc. R. Soc. London B* **1984**, *304*, 529.